Journal of Hazardous Materials 190 (2011) 613–621

Contents lists available at ScienceDirect

Journal of Hazardous Materials

journal homepage: www.elsevier.com/locate/jhazmat

Cytogenetic and genotoxic effects of zinc oxide nanoparticles on root cells of *Allium cepa*

Mamta Kumari, S. Sudheer Khan, Sunandan Pakrashi, Amitava Mukherjee, Natarajan Chandrasekaran*

Centre for Nano-Biotechnology, School of Bio-Sciences and Technology, VIT University, Vellore 632014, India

ARTICLE INFO

Article history:
Received 10 December 2010
Received in revised form 16 March 2011
Accepted 24 March 2011
Available online 6 April 2011

Keywords:
Zinc oxide nanoparticles
Allium cepa
Cytotoxicity
Genotoxicity

ABSTRACT

Increasing use of zinc oxide nanoparticles (ZnO NP) in consumer products may enhance its release into the environment. Phytotoxicity study is important to understand its possible environmental impact. *Allium cepa* (Onion bulb) is the best model organism to study genetic toxicology of nanoparticles. Here we have reported cytogenetic and genotoxic effects of ZnO NPs on the root cells of *A. cepa*. The effects of ZnO NPs on the mitotic index (MI), micronuclei index (MN index), chromosomal aberration index, and lipid peroxidation were determined through the hydroponic culturing of *A. cepa*. *A. cepa* roots were treated with the dispersions of ZnO NPs at four different concentrations (25, 50, 75, and 100 $\mu g\,ml^{-1}$). With the increasing concentrations of ZnO NPs MI decreased with the increase of pycnotic cells, on the other hand MN and chromosomal aberration index increased. The frequency of micronucleated cells was higher in ZnO NPs treated cells as compared to control (deionized distilled water). The number of cells in each mitotic phase changed upon ZnO NPs treatment. The effect of ZnO NPs on lipid peroxidation as examined by measuring TBARS concentration was evident at all the concentrations compared to bulk ZnO. The TEM image showed internalization of ZnO NPs like particles. SEM image of treated *A. cepa* demonstrated that the internalized nanoparticles agglomerated depending on the physico-chemical environment inside the cell. Our results demonstrated that ZnO NPs can be a clastogenic/genotoxic and cytotoxic agent. In conclusion, the *A. cepa* cytogenetic test can be used for the genotoxicity monitoring of novel nanomaterials like ZnO NPs, which is used in many consumer products.

1. Introduction

Zinc oxide nanoparticles (ZnO NPs) are widely used in many consumer products like cosmetics, textiles and skin lotions [1]. Usage of ZnO NPs in cosmetics [2] may bypass the usages of other nanoparticles, like nano-titanium dioxide ($nTiO_2$), because of its capacity to absorb both UV-A and UV-B radiation [3]. In fabrics, ZnO NPs are being used as an odor resistance because of its antimicrobial properties and also UV absorbent [4,5]. ZnO NPs are also used in ceramics, rubber processing, and wastewater treatment facilities [6].

The production rate of nano metal oxides for cosmetics is estimated to be 10^3 tonnes/year [5]. Worldwide production of nano zinc oxide is stated to be 528 tonnes/year [7]. The zinc oxide industry is a fragmented industry with over 300 companies around the world producing in excess of 1.2 million tonnes of ZnO per year [8].

An increased usage of ZnO NPs in many consumer products leads to their release into different environmental matrix [6]. Environmental fate and mobility of ZnO NPs strongly depended on changes in size; shape and surface chemistry of the particles varying its bioavailability [9,10]. Danovaro et al. [11] reported that 25% of the sunscreen applied on to the skin is washed off during bathing and swimming.

Historically, plants have been used as an indicator organism to study mutagenesis in higher eukaryotes. Plants system plays a critical role in the fate and transport of engineered nanoparticles in the environment, through plant uptake and bioaccumulation [12]. Plant systems have a variety of well-defined genetic endpoints including alterations in ploidy, chromosomal aberrations, and sister chromatid exchanges. The *Allium cepa* root chromosomal aberration assay is an established plant bioassay validated by the International Programme on Chemical Safety [13], and the United Nations Environment Programme [14] as an efficient and standard test for the chemical screening and in situ monitoring for genotoxicity of environmental substances.

Studies on the phytotoxicity of nanoparticles are scarce, especially with regard to its mechanisms, and on its potential uptake and subsequent fate within the food chain. ZnO NPs reduced root growth of corn and terminated root development of five plant species [15]. Lin and Xing [16] noticed that the toxicity of ZnO NPs was due to Zn^{2+} and chemical stress due to surface, size and shape

* Corresponding author. Fax: +91 416 2243092/2240411.
E-mail addresses: nchandrasekaran@vit.ac.in, nchandra40@hotmail.com (N. Chandrasekaran).

0304-3894/$ – see front matter © 2011 Elsevier B.V. All rights reserved.
doi:10.1016/j.jhazmat.2011.03.095

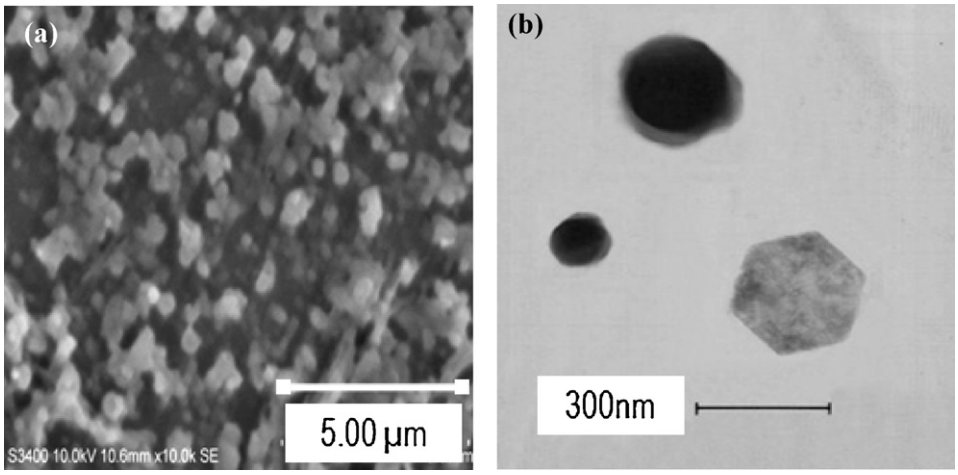

Fig. 1. (a) Scanning electron microscope (SEM) and (b) transmission electron microscope (TEM) images of ZnO NPs.

of particles. On the other hand Lin and Xing [15] found aluminum nanoparticles had no obvious effect on cucumber, but, promoted the root growth of radish and rape, and significantly retarded root elongation of ryegrass and lettuce. Specificity of nanotoxicology is still unknown. Phytotoxicity of ZnO NPs to *Arabidopsis* (member of mustard plant) was stronger, than solutions containing same concentration of soluble zinc [17]. Rye grass (*Lolium perenne*) roots showed morphological changes with high concentration ZnO NPs, i.e. root tips shrank and epidermal and cortical cells collapsed [16]. Lin and Xing [16] noticed no upward translocation of ZnO NPs from roots to shoots, i.e. ZnO NPs adhered to root surface and individual nanoparticles were observed in the apoplast and protoplast spaces in root endodermis and stele. Stampoulis et al. [18] noticed there was no negative effect when *Cucurbita pepo* seeds were grown hydroponically in ZnO NPs dispersion. ZnO NPs inhibited seed germination of rye grass and corn [15]. ZnO NPs inhibited root growth of radish and rape, when incubated in suspension of ZnO NPs [19]. However, such an inhibition was not detected while soaked in ZnO NPs suspension due to the selective permeability of seed coat [19]. Internalization of ZnO NPs was noticed in the endodermis and vascular cylinder of ryegrass roots [20].

From the results of previous nano phytotoxicological studies, it is envisaged that nanoparticles are highly selective in its toxicity response. This property could be exploited for agricultural nanotechnology. In the present study we have investigated the cytogenetic and genotoxic effects of ZnO NPs on root cells of *A. cepa*. Light microscopy, scanning electron microscopy (SEM) and transmission electron microscopes (TEM) analyses were adopted to investigate the cellular morphology, chromosomal aberrations in different stages of mitosis, and occurrence of micronucleus (MN).

2. Materials and methods

2.1. Chemicals and characterization

ZnO NPs powder and zinc oxide bulk (ZnO) were purchased from Sigma–Aldrich, USA. The physical characteristics of the ZnO NPs reported by supplier are: size < 100 nm, purity: 99.5%, and surface area 15–25 $m^2\ g^{-1}$. The physical characteristics of the ZnO bulk reported by supplier are: particle size < 5 μm, purity: 99.9%, form powder.

The morphological features of the ZnO NPs were characterized using transmission electron microscopy (Technai10, Philips) at 80 kV, and scanning electron microscopy (Hitachi, S-3400). Particle size distribution, effective diameter and polydispersity were analyzed using 90 Plus Particle Size Analyzer (Brookhaven Instruments Corporation, USA).

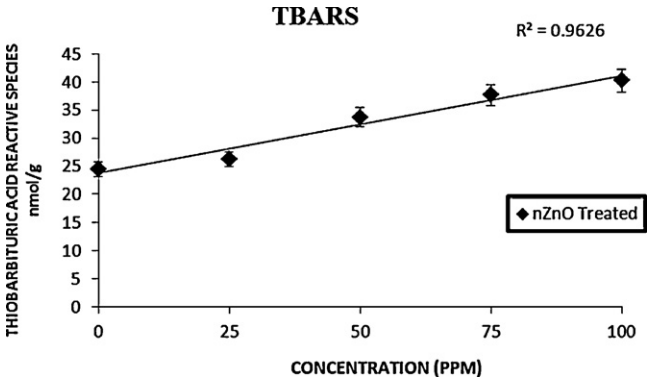

Fig. 2. Effect of ZnO NPs on the concentration of thiobarbituric acid reactive species (TBARS) in the root cells of *A. cepa*.

2.2. Preparation of nanoparticle dispersion

The ZnO NPs and ZnO bulk were suspended directly in 100 ml of Milli-Q water and dispersed by ultrasonic vibration (Sonics Vibra-Cell Ultrasonicator, VCX 130PB, 130W, 20 kHz) for 30 min to prepare four required dispersions (25 μg ml^{-1}, 50 μg ml^{-1}, 75 μg ml^{-1}, and 100 μg ml^{-1}). All concentrations were selected arbitrarily.

2.3. Metal ion concentration measurement in dispersion

The ZnO NPs dispersion was centrifuged at 12,000 rpm for 10 min. Clear supernatant was carefully collected and filtered through a 0.22 μm sterilized filter. It is a possibility that there could be some particles in the clear supernatant. The ion concentrations were measured by an atomic absorption spectrophotometer (Varian, AA240) after acidification by 1% nitric acid [16,21].

2.4. Lipid peroxidation determination

Lipid peroxidation was determined by measuring the amount of thiobarbituric acid reactive species (TBARS) according to Ohkawa et al. [22]. Each experiment was run with three replications. A total of 0.2 g of root tissues from control and ZnO NPs and ZnO

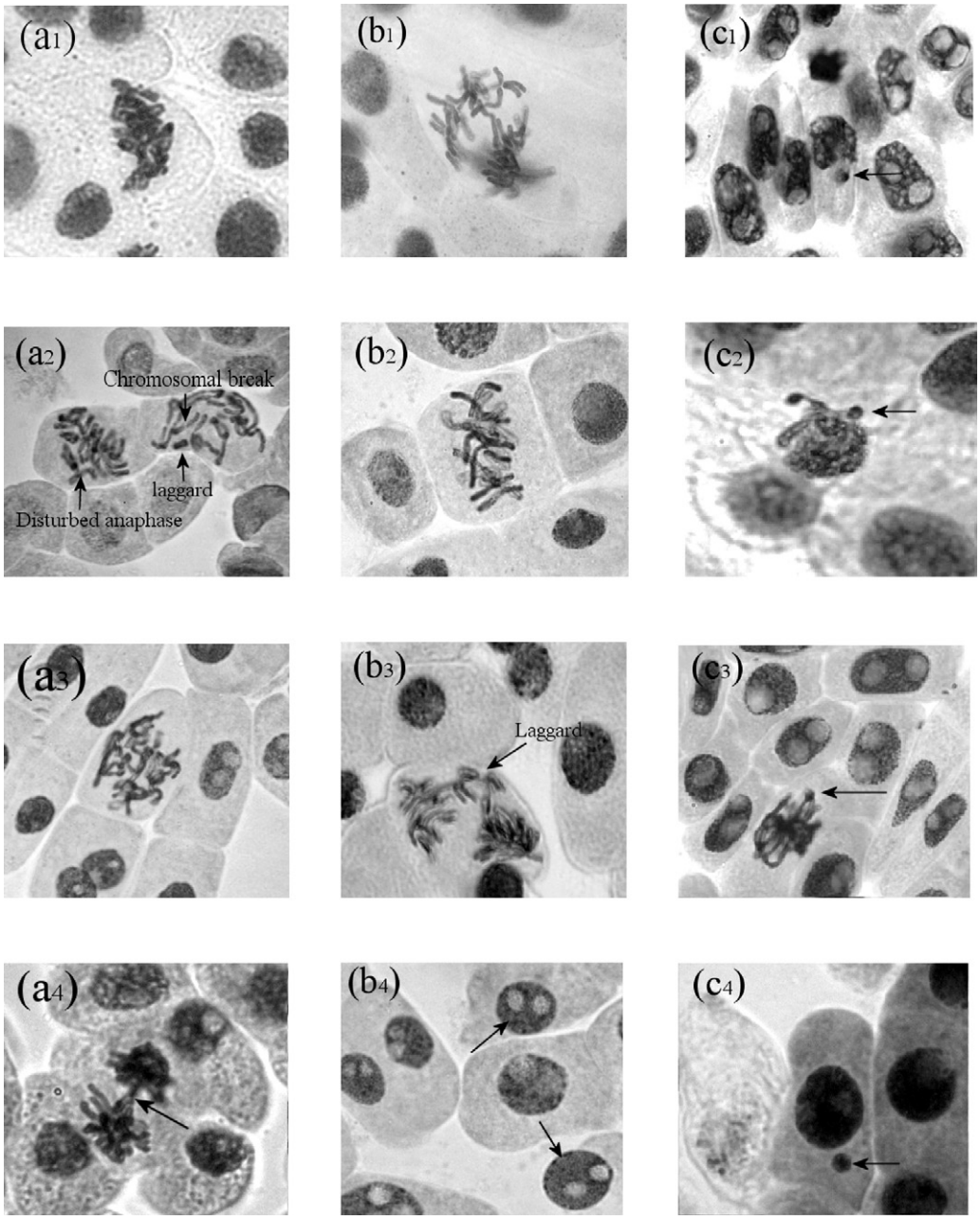

Fig. 3. Chromosomal aberrations observed in *A. cepa* meristematic cells exposed to ZnO NPs. (a_1) Sticky chromosomes in metaphase stage, (a_2) disturbed anaphase stage with chromosomal break and laggard, (a_3) disturbed metaphase, (a_4) sticky chromosomes at anaphase stage with bridge, (b_1) Multipolar anaphase, (b_2) C-mitotic cell, (b_3) vagrant chromosomes with laggard at anaphase, (b_4) binucleated cells at early prophase stage, (c_1 and c_4) prophase nuclei with micronucleus in interphase, (c_2) cell in early anaphase with chromosome adherence and budding micronucleus, (c_3) binucleated cell in early telophase with micronucleus in metaphase Magnification for all images $\times$1000.

bulk treated plants were cut into small pieces and homogenized by the addition of 1 ml of 5% trichloroacetic acid (TCA) solution. The homogenates were then transferred into fresh tubes and centrifuged at 12,000 rpm for 15 min at room temperature. Equal volumes of supernatant and 0.5% thiobarbituric acid (TBA) in 20% TCA solution (freshly prepared) were added into a new tube and incubated at 96 °C for 25 min. The tubes were transferred into ice bath and then centrifuged at 10,000 rpm for 5 min. The absorbance of the supernatant was recorded at 532 nm and corrected for non-specific turbidity by subtracting the absorbance at 600 nm; 0.5% TBA in 20% TCA solution was used as the blank. TBARS content was determined using the extinction coefficient of 155 mM^{-1} cm^{-1}.

2.5. Test system and treatment

Among the several higher plants used as test organisms, the species *A. cepa* has been used as an efficient genetic standard for environmental monitoring, since Levan's introduction of this species as test system [23–25].

Healthy onion bulbs (20–25 g) were grown in dark in a cylindrical glass beaker at room temperature (28 ± 0.5 °C) and given renewed water supply every 24 h. When the roots reached 2–3 cm in length they were treated with different concentrations of ZnO NPs and bulk ZnO suspension. The interaction time was 4 h in accordance with a protocol standardized by Fiskesjo [26].

Table 1
Occurrence of cytological effects per 1000 cells scored in *A. cepa* root cells after treatment with ZnO NPs dispersion.

Treatments	Sample size ($n=5$)	MI[a] (%)	P[b] (%)	M[c] (%)	A[d] (%)	T[e] (%)	Mean (MI%) ± S.E
Deionized distilled water	Sample 1	62.3	59.1	1.8	0.8	0.6	61.6 ± 0.31
	Sample 2	60.6	58	1.3	0.9	0.4	
	Sample 3	62.3	60.2	1.4	0.5	0.2	
	Sample 4	61.5	59.5	1.1	0.9	0	
	Sample 5	61.6	59	1.2	0.7	0.7	
ZnO NPs (25 μg ml^{-1})	Sample 1	51.5	49.6	0.9	0.7	0.3	50.4 ± 0.55
	Sample 2	48.7	47.6	0.6	0.5	0	
	Sample 3	50.5	48.6	1.1	0.6	0.2	
	Sample 4	51.7	48.4	1.3	0.7	0.3	
	Sample 5	49.8	48.8	0.7	0.3	0	
ZnO NPs (50 μg ml^{-1})	Sample 1	41.2	40.7	0.3	0.2	0	40.1 ± 0.34
	Sample 2	40.3	39.9	0.1	0.3	0	
	Sample 3	39.8	38.9	0.3	0.4	0.2	
	Sample 4	40.1	39.4	0.2	0.3	0.2	
	Sample 5	39.1	38.8	0.1	0.2	0	
ZnO NPs (75 μg ml^{-1})	Sample 1	34	33.8	0.1	0.1	0	35.3 ± 0.91
	Sample 2	33.9	33.5	0.1	0.2	0.1	
	Sample 3	36.8	36.5	0.2	0.1	0	
	Sample 4	33.6	33	0.3	0.2	0.1	
	Sample 5	38.1	37.5	0.2	0.3	0.1	
ZnO NPs (100 μg ml^{-1})	Sample 1	30.1	29.4	0.2	0.3	0.2	29.2 ± 1.19
	Sample 2	27.9	27.7	0.1	0.1	0	
	Sample 3	31.2	29.9	0.2	0.1	0	
	Sample 4	29.6	29.6	0	0	0	
	Sample 5	30.6	30.5	0.1	0	0	

[a] Mitotic index.
[b] Prophase.
[c] Metaphase.
[d] Anaphase.
[e] Telophase.

2.6. Light microscopy

The slides for microscopy were prepared following Saffranin squash technique. The root tips excised from treated and control samples were kept in 1 M HCl for about 6 min followed by staining with 40–45% Saffranin. The staining was continued for about 5–6 min. The slides were analyzed at 1000×. The mitotic index was calculated as the number of dividing cells per number of 1000 observed cells [27,28]. The number of aberrant cells was noted per total cells scored at each concentration [28,29]. The MN index was calculated following Tolbert et al. [30].

2.7. Electron microscopy

For electron microscopic analysis, *A. cepa* roots were sectioned and stained according to standard protocol [31].

2.7.1. Sample pretreatment

Sample was fixed in 3% glutaraldehyde and washed in buffer. Then it was fixed by 1% osmiumtetroxide and washed in buffer. This double fixation gives stability during dehydration, embedding and during electron bombardment. Further, it also provides staining contrast, decreased distortion; fix fine cellular ultrastructure, suitable contrast.

2.7.2. Embedding

Embedded was done in siligonised rubber mold with epoxy resin.

2.7.3. Staining for electron microscopy

The embedded mold was kept in incubator (60 °C) for polymerization. After cooling one micron thick sections was cut through ultra microtome (Leica ultracut UCT) with glass knife and stained by toluidine blue. Ultrathin section (below 100 nm) was cut through ultramicrotome (Leica) with diamond knife (diatome). The sections are taken on a copper grid and stained with double metallic uranyl acetate and Reynold's solution (sodium citrate + lead nitrate), which gives contrast to the section. The section was analyzed under electron microscope (Philips 2010, The Netherland).

2.8. Data treatment

Different phases of mitosis were counted and chromosomal abnormalities were observed to calculate mitotic index, phase indices and total abnormality percentage at different phases of cell division. Based on the observations the following indices were calculated in order to quantify the effect of ZnO NPs [32,33].

$$\text{Mitotic index(MI)} = \frac{T_{DC}}{T_C} \times 100 \quad (1)$$

$$\text{Phase index(PI)} = \frac{T_C}{T_{DC}} \times 100 \quad (2)$$

$$\text{Total percentage of abnormal cells} = \frac{T_{abn}}{T_{DC}} \times 100 \quad (3)$$

$$\text{MN index(\%)} = \frac{T_{MN}}{T_{BN}} \times 100 \quad (4)$$

where T_{DC} = total no. of dividing cells; T_C = total no. cells observed; T_{abn} = total no. of abnormal cells; T_{MN} = total no. of micronucleus observed; T_{BN} = total no. of binucleated cells observed [28].

Table 2
Chromosomal aberrations and micronuclei index of ZnO NPs treated cells of *A. cepa.* (1000 cells were scored for each sample and each treatment groups have 5 samples).

Treatments	Number of sample ($n = 5$)	Chromosome aberrations					Chromosomal aberration index (%)	Micronucleus				Micronuclei index (%)
		Sticky	Bridge at anaphase	c-mitosis	Multipolar	Vagrant		Interphase	Anaphase	Metaphase	Telophase	
(De-ionized distilled water)	Sample 1	–	–	–	–	–	Nil	–	–	–	–	2.05 ± 0.98
	Sample 2	–	–	–	–	–		–	–	–	–	
	Sample 3	–	–	–	–	–		–	–	–	–	
	Sample 4	–	–	–	–	–		–	–	–	–	
	Sample 5	–	–	–	–	–		–	–	–	–	
ZnO NPs (25 μg ml^{-1})	Sample 1	+	–	–	–	–	0.7	+	+	–	–	8.9 ± 0.45
	Sample 2	+	–	–	–	–		–	–	–	–	
	Sample 3	–	–	–	–	–		+	–	–	–	
	Sample 4	+	–	–	–	–		–	–	–	–	
	Sample 5	+	–	–	–	–		–	–	–	–	
ZnO NPs (50 μg ml^{-1})	Sample 1	+	–	–	–	–	1.3	+	+	–	+	9.2 ± 0.98
	Sample 2	+	–	–	–	–		+	+	–	–	
	Sample 3	+	–	–	–	–		–	–	–	–	
	Sample 4	+	–	–	–	–		+	–	–	–	
	Sample 5	+	–	–	–	+		–	–	–	–	
ZnO NPs (75 μg ml^{-1})	Sample 1	+	–	–	+	–	2.3	–	+	–	+	15.6 ± 1.31
	Sample 2	+	+	–	–	–		–	+	–	+	
	Sample 3	+	–	+	–	+		+	+	+	+	
	Sample 4	+	–	–	–	–		+	–	–	–	
	Sample 5	+	+	–	–	+		–	–	–	–	
ZnO NPs (100 μg ml^{-1})	Sample 1	+	–	–	–	–	4.2	+	+	–	+	18.7 ± 1.2
	Sample 2	+	–	+	+	–		+	–	–	+	
	Sample 3	+	–	–	–	–		+	–	+	–	
	Sample 4	+	–	–	–	–		–	+	–	–	
	Sample 5	+	+	+	+	+		–	–	–	–	

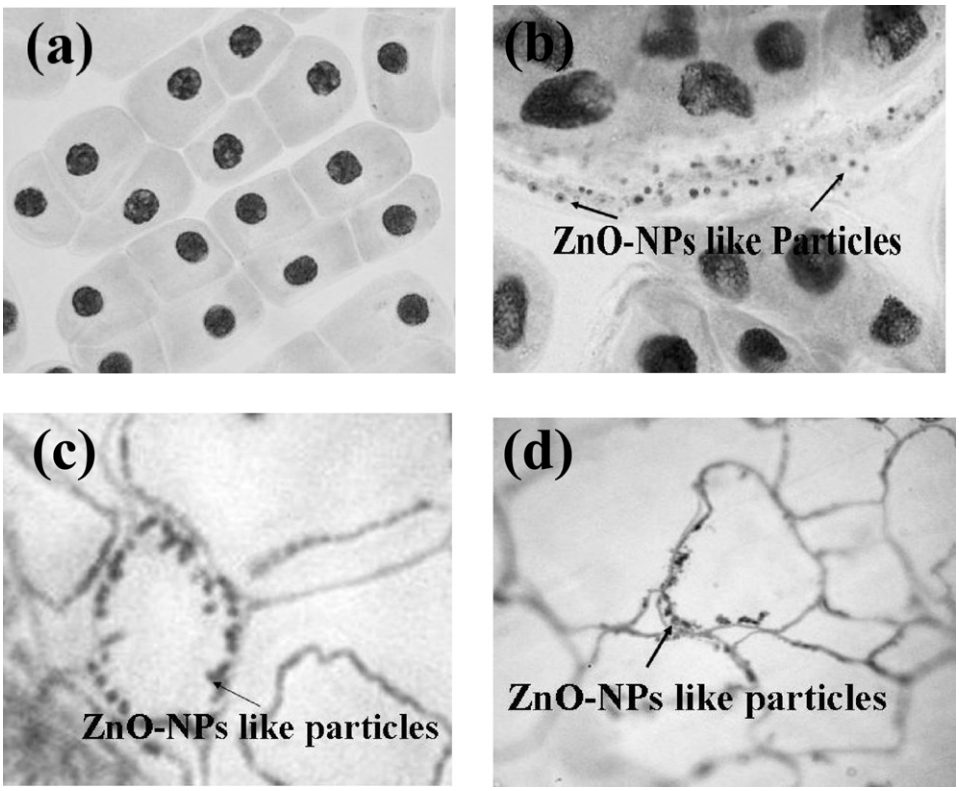

Fig. 4. *A. cepa* root cells. (a) Light microscopy image of control (treated with distilled water) (b) light microscopy image of ZnO NPs treated (100 μg ml^{-1}) root cells showing agglomeration of particles between the cell membranes. (c) Cross section of *A. cepa* roots showing agglomeration of particles on the outer surface of epidermal cell wall (d) phase contrast image showing particle aggregation in the cell interior. Magnification for all images ×1000.

3. Results

3.1. Physicochemical characterization of ZnO NPs

The high-resolution SEM image of procured ZnO NPs (Fig. 1a and TEM image (Fig. 1b) showed that the particles were nearly spherical to hexagonal shaped (100 nm). The hydrodynamic diameter of ZnO NPs (<100 nm) in Milli-Q water was determined by dynamic light scattering (DLS) at 25 °C. After dispersion of ZnO NPs in Milli-Q water, the effective diameter was found to be 120 ± 2.6 nm. The surface area was 21 m^2 g^{-1}. The polydispersity was 0.225.

The zinc ion (Zn^{2+}) concentration measured in the ZnO NPs dispersions of 25, 50, 75, 100 μg ml^{-1} by AAS were 9.5 μg ml^{-1}, 25 μg ml^{-1}, 20.7 μg ml^{-1}, 31.9 μg ml^{-1}, 43.7 μg ml^{-1}, respectively.

3.2. Lipid peroxidation

The effect of ZnO NPs on lipid peroxidation was examined by measuring TBARS concentration. The TBARS concentration for 25, 50, 75, and 100 μg ml^{-1} ZnO NPs treated samples were noted to be 26.2, 33.7, 37.7, and 40.2 nmol g^{-1}, respectively (Fig. 2). On the other hand ZnO bulk treated samples showed TBARS concentrations as 24.8, 25.9, 27.3, and 31.5 nmol g^{-1} for 25, 50, 75, and 100 μg ml^{-1} concentration of ZnO bulk, respectively.

3.3. Microscopic analysis

The effect of the ZnO NPs in the root cells of *A. cepa* is shown in Fig. 3. Results of the cytological and chromosomal aberrations observed in the root tip cells of *A. cepa* treated with different concentrations of ZnO NPs are shown in Tables 1 and 2. Cell cycle analysis showed that the percentage of cells in the different phases of mitosis (prophase, metaphase, anaphase and telophase) decreased with increasing ZnO NPs dispersions when compared to the control. Prophase percentage changed rapidly with a similar result as that seen for the mitotic indices.

The mitotic index (MI) for the samples treated with 25, 50, 75 and 100 μg ml^{-1} ZnO NPs was 50.4%, 40.1%, 35.3% and 29.2%, respectively. In the case of control, it was 61.6%. No chromosomal aberration was observed in the control. The chromosomal aberration index for 25, 50, 75 and 100 μg ml^{-1} ZnO NPs treated *A. cepa* root cells showed 0.52%, 1.52%, 2.74% and 4.12%, respectively. The MN index for 25, 50, 75 and 100 μg ml^{-1} ZnO NPs treated *A. cepa* root cells showed 8.7%, 9.2%, 15.6% and 18.7%. Dose dependent decrease in MI, increase of chromosomal aberration, and MN was observed.

We also studied the toxicity of ZnO bulk particles in the same test concentration ranges (25 μg ml^{-1}, 50 μg ml^{-1}, 75 μg ml^{-1} and 100 μg ml^{-1}) to the *A. cepa* root system. The MI was 48.7% for *A. cepa* treated with 100 μg ml^{-1} ZnO bulk compared to 29.2% for ZnO NPs treated samples.

The dissolved metal ions in the ZnO NPs dispersion detected by AAS was: 9.5 μg ml^{-1} Zn^{+2} in the 25 μg ml^{-1} dispersion; 20.7 μg ml^{-1} Zn^{+2} in the 50 μg ml^{-1} dispersion; 31.9 μg ml^{-1} Zn^{+2} in the 75 μg ml^{-1} dispersion and 43.7 μg ml^{-1} Zn^{+2} in the 100 μg ml^{-1} dispersion.

To determine the effect of zinc ions (Zn^{2+}) present in supernatant of the ZnO NP dispersion, the toxicity to the *A. cepa* roots was examined at 9.5, 20.7, 31.9 and 43.7 μg ml^{-1} zinc ions (Zn^{2+}) concentrations. The MI was 35.7% for *A. cepa* treated with 43.7 μg ml^{-1} of zinc ions (Zn^{2+}), compared to 29.2% for ZnO NPs treated samples. No micronucleus was observed in the case of zinc ions (Zn^{2+}) treated *A. cepa*.

As shown in the representative microscopic images given in Fig. 3a–c, five main types of chromosome aberrations were recorded in anaphase–teleophase: stickiness, bridges, vagrant

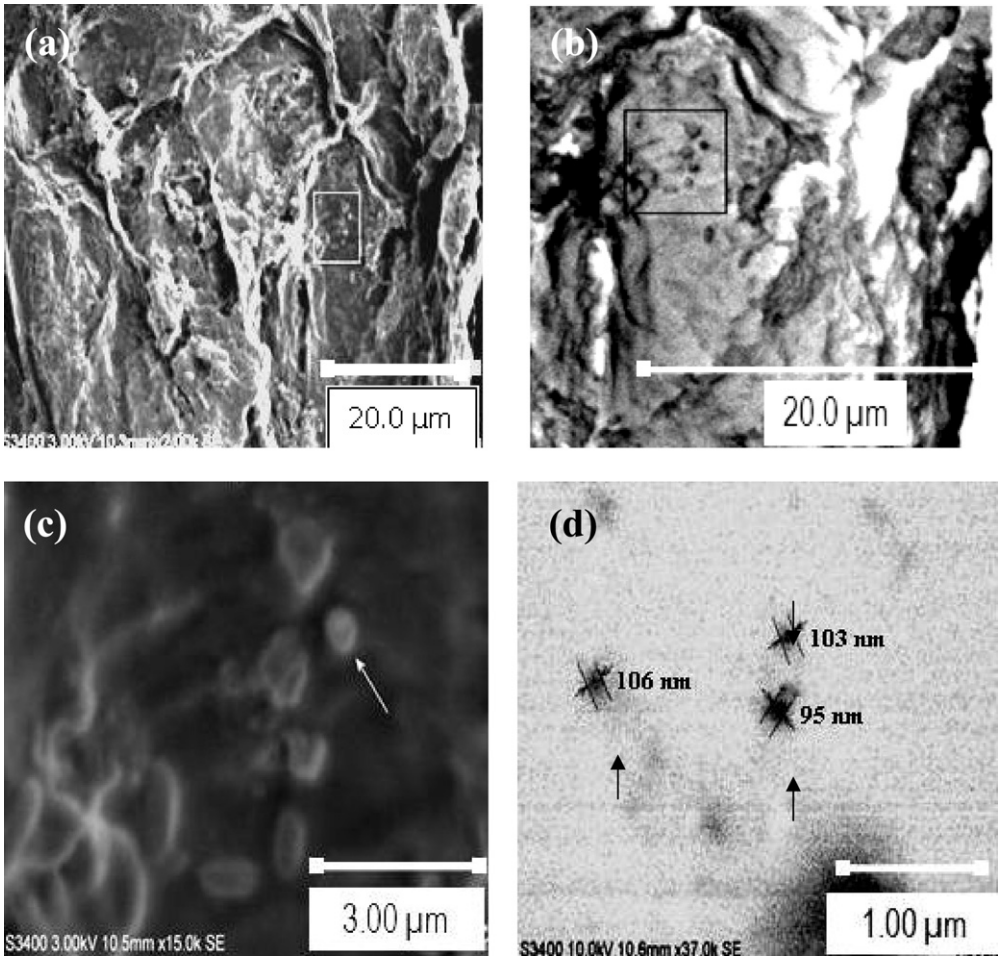

Fig. 5. SEM images of *A. cepa* root cells treated with 100 μg ml^{-1} ZnO NPs showing the presence of particles in intracellular matrix; (d) ZnO NPs treated root cells showing particles in the size range of 95, 103 and 106 nm. Magnification for images (a) ×15,000, (b), (c) and (d) ×30,000.

chromosomes, multipolarity and fragments. For 50 μg ml^{-1} concentration, we observed chromatin bridge, stickiness, and disturbed metaphase; for 75 μg ml^{-1} vagrant chromosome, chromosomal break and for 100 μg ml^{-1}, binucleated cells, complete disintegration of cell walls, nuclear membrane disruption, bridge at anaphase, vagrant chromosomes were observed. MN was observed in all the concentration of ZnO NPs treated samples.

ZnO NPs treated *A. cepa* showed clear disintegration of cellular matrix, and structural deformation compared to control Fig. 4. There was a chain of particles like deposits in cellular matrix for the 100 μg ml^{-1} ZnO NPs treated cells (Fig. 4b–d).

Deposits of ZnO NPs like particles were noted in the SEM images of the *A. cepa* treated with 100 μg ml^{-1} ZnO NPs (Fig. 5). Fig. 5a–c showed ZnO NPs like particles inside root cells of *A. cepa*. Fig. 5d showed ZnO NPs like particles in the cellular matrix. Their sizes were 95, 103 and 106 nm. TEM images of *A. cepa* roots treated with 100 μg ml^{-1} ZnO NPs showed presence of nanoparticles in the cell membrane. Agglomerations of particles were seen in the cytoplasmic matrix (Fig. 6).

4. Discussion

Our results demonstrated that exposure of *A. cepa* roots to ZnO NPs causes cytotoxicity and genotoxicity. There was concentration dependent inhibition of mitotic index, which indicated cytotoxic potential of ZnO NPs in *A. cepa* [34,35]. Similar effects on MI were described in our previous publication [28]. The decrease in mitotic activity probably indicates mitodepressive effect of ZnO NPs, i.e. it could interfere with the normal development of mitosis, thus preventing a number of cells from entering the prophase and blocking the mitotic cycle during interphase inhibiting DNA/protein synthesis [36].

The percentage of total chromosome aberrations increased with increasing the test concentration. Even at 100 μg ml^{-1} ZnO NPs the mitotic index was not blocked by the effect of ZnO NPs. If 100 μg ml^{-1} was too toxic, it might have caused cell death, and interfere with the scoring of cells for aberrations caused by ZnO NPs. The percentage of chromosome aberrations was not diminished. Among these aberrations, sticky chromosomes were the most frequently observed aberration at anaphase–telophase stages of mitosis in root tips of *A. cepa* treated with ZnO NPs (Fig. 3). Sticky chromosomes are considered to be a chromatid type of aberration [37]. Darlington and Mc-Leish [38] suggested that stickiness might be due to degradation or depolymerization of chromosomal DNA.

In addition to the types of chromosome aberrations induced in the anaphase–telophase cells, the formation of micronucleus in the interphase cells was noted. The percentage of micronucleated cells was higher at 100 μg ml^{-1} ZnO NPs treated *A. cepa*. The induction of MN in root meristem cells of *A. ce*pa is the manifestation of fragments or vagrant chromosomes [39].

SEM images of *A. cepa* root cells showed ZnO NPs like deposits inside the cell matrix in size range around 100 nm (Fig. 5). TEM images (Fig. 6) also confirmed internalization of the nanoparticles, agglomerated particles (around 150 nm size) can be observed in Fig. 6e. On entering the cells, the nanoparticles are transported from one cell to other through plasmadesmata, during this process,

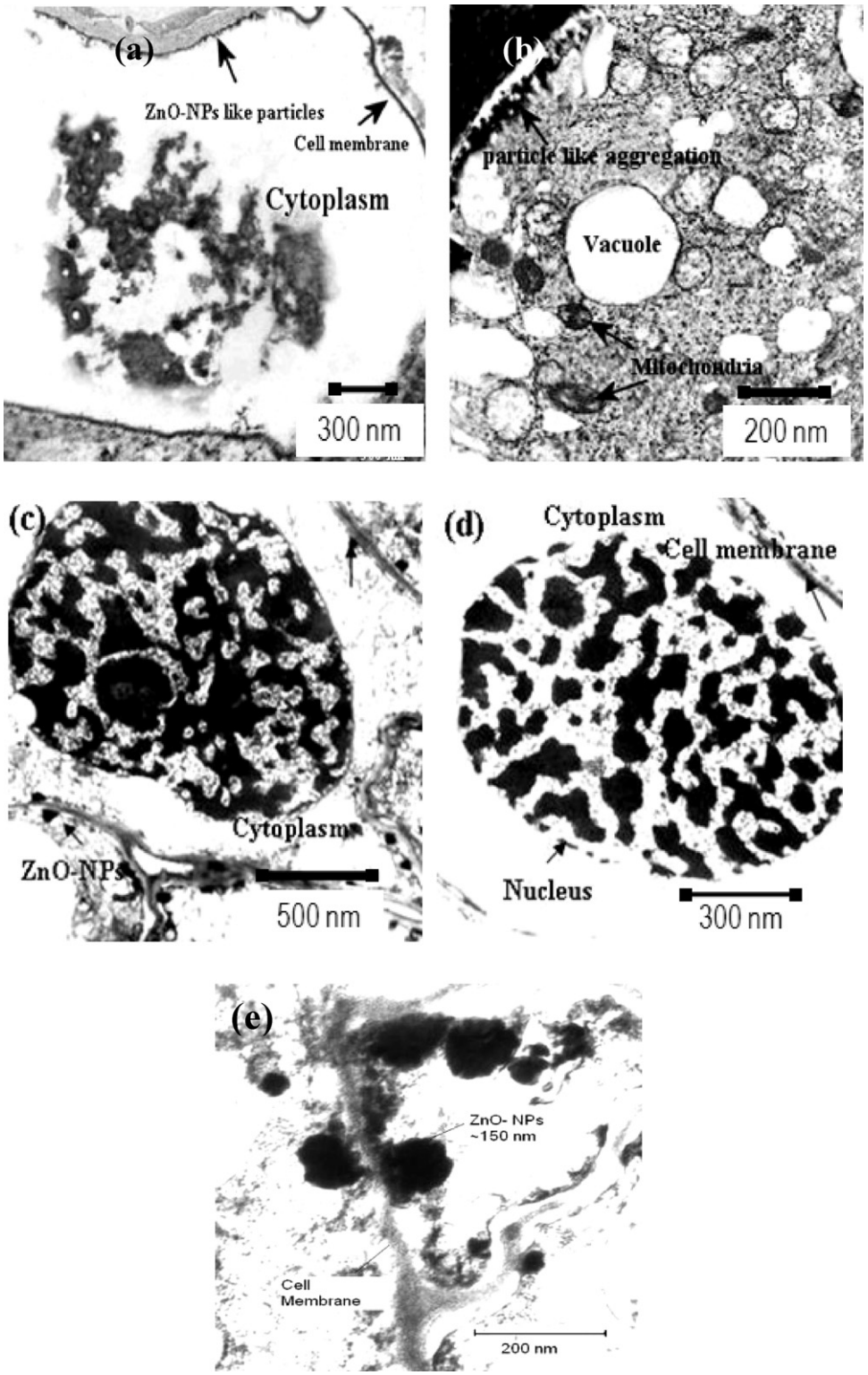

Fig. 6. TEM images of *A. cepa* root cells treated with 100 μg ml^{-1} ZnO NPs; (a) ZnO NPs treated root cells showing the presence of nanoparticles around the cell membranes and the cytoplasm; (b) ZnO NPs treated root cells showing the presence of particles at the inner side of cell membrane (c) ZnO NPs treated root cells showing the presence of nanoparticles around cell membrane, in the cytoplasm and deformed nucleus (d) control sample treated with Milli-Q water showing no nanoparticles around cell membrane and in the cytoplasm, (e) ZnO NPs treated root cells showing aggregation of nanoparticles around cell membrane, in the cytoplasm, with a size of 150 nm. Magnification for images (a) 15,000×, (b) 10,000×, (c) 4500×, (d) 4500× and (e) ×45,000.

aggregation of nanoparticles may happen resulting in increasing size of the nanoparticles [19].

Metal oxide toxicity to *A. cepa* could also be induced by dissolved metal ions from the oxides. Brunner et al. [40] studied the toxicity of nanoparticles to a human and a rodent cell lines. They divided the tested nanoparticles into soluble and insoluble nanoparticles, suggesting that the toxicity of nanoparticles was due to soluble metal ions released from nanoparticles before or after the nanoparticles

enter the cell. Our results indicated that toxicity of ZnO NPs to *A. cepa* was not due to dissolved zinc ions alone. The higher toxicity of ZnO NPs, as compared to Zn^{2+} ions present in dispersion was likely due to higher intrinsic toxicity of ZnO NPs. In the case of treatments with micron sized bulk ZnO particles no micronucleus was observed in contrast to treatments with ZnO NPs. These results bring out the stark contrast in toxic behavior of micron and nano sized ZnO particles hinting at probable intrinsic nano size related effects. Our findings corroborate the findings of Jiang et al. [41] that ZnO NPs toxicity to bacterial species was much higher than the ZnO bulk, and zinc ions toxicity.

The possible mechanism, for higher intrinsic toxicity of ZnO NPs to *A. cepa* could be the release of reactive oxygen species (ROS). ROS could convert fatty acids to toxic lipid peroxides, destroying biological membranes. This causes the TBARS formation, damaging membrane permeability. TBARS formation is used as the general indicator of the extent of lipid peroxidation resulting from oxidative stress [42]. This was supported by our findings, on the increase of TBARS formation at all concentrations of ZnO NPs and ZnO bulk treated to *A. cepa*. However, higher concentrations of TBARS were formed in ZnO NPs treated *A. cepa* compared to their bulk counterparts. This was parallel to the findings of Lin et al. [43] observed TBARS increased in epithelial cells by 170% and 145% after exposure to 14 $\mu g\,ml^{-1}$ of 70 and 420 nm ZnO NPs particles for 24 h, respectively; 70 nm ZnO NPs induced a higher TBARS level than that of 420 nm ZnO NPs.

Therefore, higher toxicity of ZnO NPs to *A. cepa* in causing chromosomal aberrations, cellular dysfunctions, and MN formation would be due more to the nano size forms of the material than its ions or bulk size forms.

Acknowledgement

This study was supported by the Chancellor, VIT University. The authors also thank VIT University Management for providing financial support towards Nanotoxicology program.

References

[1] C.T. Ng, J.J. Li, B.H. Bay, L.Y.L. Yung, Current studies into the genotoxic effects of nanomaterials, J. Nucleic Acids (2010), doi:10.4061/2010/947859.
[2] V. Sharma, R.K. Shukla, N. Saxena, D. Parmar, M. Das, A. Dhawan, Zinc oxide nanoparticles in sunscreen can damage skin DNA, Toxicol. Lett. 185 (2009) 211–218.
[3] D.T. Tran, R. Salmon, Potential photocarcinogenic effects of nanoparticle sunscreens, Australas. J. Dermatol. 52 (2011) 1–6.
[4] A. Becheri, M. Durr, P. Lo Nostro, P. Baglioni, Synthesis and characterization of zinc oxide nanoparticles: application to textiles as UV-absorbers, J. Nanopart. Res. 10 (2008) 679–689.
[5] C.A. Clausen, F. Green III, S.N. Kartal, Weatherability and leach resistance of wood impregnated with nano-zinc oxide, Nanoscale Res. Lett. 5 (2010) 1464–1467.
[6] G. Ghodake, Y.D. Seo, D.S. Lee, Hazardous phytotoxic nature of cobalt and zinc oxide nanoparticles assessed using *Allium cepa*, J. Hazard. Mater. 186 (2011) 952–955.
[7] S. Zhang, H. Saebfar, Chemical information call-in candidate: nano zinc oxide, California Dept. of Toxic substances control, September, 2010, pp. 1–11 (http://www.dtsc.ca.gov/TechnologyDevelopment/Nanotechnology/upload/Nano_Zinc_Oxide.pdf).
[8] International Zinc Association, ZincOx Resources plc, http://www.znox.com/industry/zinc-oxide.asp.
[9] K.G. Scheckel, T.P. Luxton, A.M. El Badawy, C.A. Impellitteri, T.M. Tolaymat, Synchrotron speciation of silver and zinc oxide nanoparticles aged in a kaolin suspension, Environ. Sci. Technol. 44 (2010) 1307–1312.
[10] E. Navarro, A. Baun, R. Behra, N.B. Hartmann, J. Filser, A.J. Miao, A. Quigg, P.H. Santschi, L. Sigg, Environmental behavior and ecotoxicity of engineered nanoparticles to algae, plants, and fungi, Ecotoxicology 17 (2008) 372–386.
[11] R Danovaro, L. Bongiorni, C. Corinaldesi, D. Giovannelli, E. Damiani, P. Astolfi, L. Greci, A. Pusceddu, Sunscreens cause coral bleaching by promoting viral infections, Environ. Health Perspect. 116 (2008) 441–447.
[12] R.C. Monica, R. Cremonini, Nanoparticles and higher plants, Cryologia 62 (2009) 161–165.
[13] WHO, Guide to short-term tests for detecting mutagenic and carcinogenic chemicals, in: Environment Health Criteria 51, WHO, Geneva, 1985, pp. 208.
[14] W.F. Grant, Chromosome aberration assays in *Allium*: a report of the U.S. environmental protection agency gene-tox program, Mutat. Res. Rev. Genet. Toxicol. 99 (1982) 273–291.
[15] D. Lin, B. Xing, Phytotoxicity of nanoparticle: inhibition of seed germination and root growth, Environ. Pollut. 150 (2007) 243–250.
[16] D. Lin, B. Xing, Root uptake and phytotoxicity of ZnO nanoparticles, Environ. Sci. Technol. 42 (2008) 5580–5585.
[17] C.W. Lee, S. Mahendra, K. Zodrow, D. Li, Y.C. Tsai, J. Braam, Developmental phytotoxicity of metal oxide nanoparticles to *Arabidopsis thaliana*, Environ. Toxicol. Chem. 29 (2010) 669–675.
[18] D. Stampoulis, S.K. Sinha, J.C. White, Assay-dependent phytotoxicity of nanoparticles to plants, Environ. Sci. Technol. 43 (2009) 9472–9479.
[19] R. Nair, S.H. Varghese, B.G. Nair, T. Maekawa, Y. Yoshida, D.S. Kumar, Nanoparticulate material delivery to plants, Plant Sci. 179 (2010) 154–163.
[20] X. Ma, J.G. Lee, Y. Deng, A. Kolmakov, Interactions between engineered nanoparticles (ENPs) and plants: phytotoxicity, uptake and accumulation, Sci. Total Environ. 408 (2010) 3053–3061.
[21] H.H. Wang, R.L. Wick, B.S. Xing, Toxicity of nanoparticles and bulk ZnO, Al_2O_3 and TiO_2 to the nematode *Caenorhabditis elegans*, Environ. Pollut. 157 (2009) 1171–1177.
[22] H. Ohkawa, N. Ohishi, Y. Yagi, Assay of lipid peroxides in animal tissue by thiobarbituric acid reaction, Anal. Biochem. 95 (1979) 351–358.
[23] A. Levan, The effect of colchicine on root mitosis in *Allium*, Hereditas 24 (1938) 471–486.
[24] Royal Swedish Academy of Sciences, Evaluation of genetic risks of environmental mutagens, Environ. Health Prospect. 27 (1973) 3–6.
[25] H.F. Stich, P. Lam, L.W. Lo, D.J. Koropatnick, H.C. San, The search for relevant short-term biassays for chemical carcinogens: the tribulation of a modern sisyphus, Can. J. Genet. Cytol. 17 (1975) 471–492.
[26] G. Fiskesjo, The *Allium* test as a standard in environmental monitoring, Hereditas 102 (1985) 99–112.
[27] G. Fiskesjo, *Allium cepa* test for screening chemicals; evaluation of cytologic parameters, in: W. Wang, J.W. Gorsuch, J.S. Hughes (Eds.), Plants for Environmental Studies, Lewis Publishers Ltd., New York, 1997, p. 308.
[28] M. Kumari, A. Mukherjee, N. Chandrasekaran, Genotoxicity of silver nanoparticles in *Allium cepa*, Sci. Total Environ. 407 (2009) 5243–5246.
[29] A.A. Bakare, A.A. Mosuro, O. Osibanjo, Effect of simulated leachate on chromosomes and mitosis in roots of *Allium cepa* (L), J. Environ. Biol. 21 (2000) 263.
[30] P.E. Tolbert, C.M. Shy, J.W. Allen, Micronuclei and other nuclear abnormalities in buccal smears, method and development, Mutat. Res. 271 (1992) 69–71.
[31] M. Wierzbicka, Lead in the apoplast of *Allium cepa* L. root tips-ultrastructural studies, Plant Sci. 133 (1998) 105–119.
[32] P. Bhatta, S.R. Sakya, Study of mitotic activity and chromosomal behaviour in root meristem of *Allium cepa* L. treated with magnesium sulphate, Ecological Society (ECOS), EOPRINT 15 (2008) 83–88, ISSN 1024-8668 Nepal, www.ecosnepal.com.
[33] M Fenech, The *in vitro* micronucleus technique, Mutat. Res. 455 (2000) 81–95.
[34] K. Linnainma, T. Meretoj, M. Sors, H. Vainto, Cytogenetic effects of styrene and styrene oxide, Mutat. Res. 58 (1978) 277–286.
[35] L. Marcano, I. Carruyo, A. Del-Campo, X. Montiel, Cytotoxicity and mode of action of maleic hydrazide in root tips of *Allium cepa* L, Environ. Res. 94 (2004) 221–226.
[36] A.A. Elghamery, A.I. Elnahas, M.M. Mansour, The action of atrazine herbicide as an inhibitor of cell division on chromosomes and nucleic acids content in root meristems of *Allium cepa* and *Vicia faba*, Cytologia 55 (2000) 209–215.
[37] A. Badr, Effect of the s-triazine herbicide terbutryn on mitosis chromosomes and nucleic acids in root tips of *Vicia faba*, Cytologia 51 (1986) 571–578.
[38] C.D. Darlington, L. Mc-Leish, Action of maleic hydrazide on the cell, Nature 167 (1951) 407–408.
[39] H. Yi, Z. Meng, Genotoxicity of hydrated sulfur dioxide on root tips of *Allium sativum* and *Vicia faba*, Mutat. Res. 537 (2003) 1091124.
[40] T.J. Brunner, P. Wick, P. Manser, P. Spohn, R.N. Grass, L.K. Limbach, A. Bruinink, W.J. Stark, In vitro cytotoxicity of oxide nanoparticles: comparision to asbestos, silica, and the effect of particle solubility, Environ. Sci. Technol. 40 (2006) 4374–4381.
[41] W. Jiang, H. Mashayekhi, B. Xing, Bacterial toxicity comparison between nano- and micro-scaled oxide particles, Environ. Pollut. 157 (2009) 1619–1625.
[42] H.A. Jeng, J. Swanson, Toxicity of metal oxide nanoparticles in mammalian cells, J. Environ. Sci. Health 41 (2006) 2699–2711.
[43] W. Lin, Y. Xu, C.C. Huang, Y. Ma, K.B. Shannon, D.R. Chen, Y.W. Huang, Toxicity of nano- and micro-sized particles in human lung epithelial cells, J. Nanopart. Res. 11 (2009) 25–39.